Dalton Transactions

Accepted Manuscript

ROYAL SOCIETY OF CHEMISTRY

www.rsc.org/dalton

Cite this: DOI: 10.1039/c0xx00000x

www.rsc.org/xxxxxx

ARTICLE TYPE

Series of open-framework aluminoborates containing $[B_5O_{10}]$ clusters

Li Wei,[a] Guo-Ming Wang[b,]*, Huan He,[a] Bai-Feng Yang,[a] Guo-Yu Yang*[a,c]

Received (in XXX, XXX) Xth XXXXXXXXX 20XX, Accepted Xth XXXXXXXXX 20XX
DOI: 10.1039/b000000x

Three new open-framework aluminoborates (ABOs), $Rb_2AlB_5O_{10}·4H_2O$ (**1**), $[C_5N_2H_{16}]AlB_5O_{10}$ (**2**, $C_5N_2H_{16}$ = *N*-ethyl-1,3-diaminopropane) and $[H_2dap][(CH_3)_2NH]AlB_5O_{10}$ (**3**, dap = 1,2-diaminopropane) have been made under solvothermal conditions and characterized by elemental analysis, IR, TGA, UV-Vis, powder XRD, single crystal XRD, fluorescence spectra and NLO determination, respectively. These three ABOs display two structural types: **1** and **2** are isostructural and crystallize in acentric space groups $C222_1$ and $P2_12_12_1$ respectively, showing intersecting helical channels and good NLO properties; while **3** crystallizes in the centrosymmetric space group *Pbca* and has CrB_4 topology, exhibiting intersecting 8-, 11- and 14-ring channels. UV-vis spectral investigation indicates that they are wide-band-gap semiconductors.

Introduction

The current increasing interest in designing and making crystalline borate materials has been significantly provoked not only by their diverse structural chemistry but also by their promising applications in mineralogy, luminescence and nonlinear optical (NLO) properties.[1] From the perspective of structure, the success of borates can be attributed to the flexibility of boron to adopt both BO_3 and BO_4 coordination modes, together with the propensity of such groups to polymerize into a wide range of oxo-borate clusters.[2] More importantly, boron-containing materials have an increased tendency to crystallize in acentric space groups. For example, compared to only 15% of inorganic crystals crystallizing in acentric space groups, more than 35% of known borates are featured with acentric structures.[3] The most well-known example is the discovery of β-BaB_2O_4 (BBO), which exhibits excellent excellent NLO property and wide use in industry.[4] Subsequently, some important alkali/ alkaline-earth metal NLO borate materials, such as LiB_3O_5 (LBO) CsB_3O_5 (CBO), $Sr_2Be_2B_2O_7$ (SBBO), etc., have also been achieved in this family.[5]

Recently, attempts to introduce heteroatoms into nonmetal borate backbones for making novel open frameworks has result in some intriguing systems, such as B-P-O,[6] B-O-Zn,[7] B-O-Ge[8] and B-O-V,[9] etc. Al is a special element and in the same group of B and also has flexible coordination modes (AlO_4: tetrahedral, AlO_5: square-pyramidal or trigonal-bipyramidal, and AlO_6: octahedral). Since the discovery of Al in natural zeolites, it has been widely used in making numerous artificial zeolites.[10] Therefore, it is highly expected that open framework aluminoborates (ABOs) may integrate zeolitic porosity with the extraordinary optical properties of borate materials. However, to the best of our knowledge, the progress in the porous ABOs system is still in its infant stage, and only very limited ABOs have been reported to date. Using boric acid flux method, for example, Lin et al. realized two open-framework ABOs of PKU-1 and PKU-2 with extra-large pores of 18- and 24-ring channels.[11e,f] More recently, applying mild hydro(solvo)thermal synthetic routes, we have successfully made a series of ABOs with diverse oxoboron clusters and excellent NLO properties.[12] In these ABOs, the various shapes, sizes, and charges of protonated organic amines, inorganic cations or metal complexes have played the role of structure directing agent in the formation of various topological frameworks. However, the detailed reaction mechanism of templating species in most hydrothermal reactions is essentially unknown, and the synthesis of such solid still retains plenty of exploratory work at the present stage. In addition to the pursuit of new NLO materials, the main purpose of our group in the study of ABOs system is focused on the influence of various templates on the inorganic compositions and topologies of resulting open-framework structures. In exploration of this theme, three new 3D aluminoborates containing the same $[B_5O_{10}]$ cluster have been realized: $Rb_2AlB_5O_{10}·4H_2O$ (**1**), $[C_5N_2H_{16}]AlB_5O_{10}$ (**2**) and $[H_2dap][(CH_3)_2NH]AlB_5O_{10}$ (**3**) ($C_5N_2H_{16}$ = *N*-ethyl-1,3-diamino-propane, dap = 1, 2-diaminopropane). Structures **1** and **2** are acentric with intersecting helical channels, and present good NLO activities. Although **3** is centrosymmetric and has no NLO property, its structure features intersecting 14- and 8-ring channels, as well as multinational large odd 11-ring channels.

Experimental

Materials and instrumentation

All chemicals were purchased from commercial sources and used without further purification. The IR spectra (KBr pellets) were recorded on a Nicolet iS10 spectrophotometer over a range 400-4000cm^{-1}. Thermogravimetric analyses (TGA) were performed on a METTLER TOLEDO TGA//DSC1/1100 analyzer under an air atmosphere with a heating rate of 10°C min^{-1}. XRD powder patterns were collected on a Bruker D8 ADVANCE X-ray diff-

ractometer using graphite-monochromated Cu Kα_1 radiation (λ = 1.54056Å). The UV-vis-NIR transmittance spectra were recorded at room temperature on a computer-controlled Shimadzu UV-3600 spectrophotometer equipped with an integrating sphere. Fluorescence spectral analyses were performed on a Perkin Elmer LS55 fluorescence spectrometer. The elemental analyses for C, H, and N were carried out on an Elemental Vario EL *III* elemental analyzer. The measurement of the powder frequency-doubling effect was carried out on the sieved powder of compound by means of the Kurtz and Perry method.[13] The fundamental wave-length was 1064 nm and was generated by a Q-switched Nd:YAG laser. The SHG wavelength was 532 nm. KDP powder was used as a reference.

Preparation of $Rb_2AlB_5O_{10}\cdot4H_2O$ (1)

A mixture of Al(*i*-PrO)$_3$ (0.204 g), H_3BO_3 (0.370 g), $RbCl_2$ (0.120 g) was added to H_2O (1.0mL), alcohol(1.0 mL) and methylamine alcohol solution (MAS, 5 mL, V(CH_3NH_2): V(CH_3-CH_2OH) = 1: 2), then 2-methyl-1,5-pentanediamine ($NH_2(CH_2)_3$-$CH(CH_3)CH_2NH_2$, 0.5 mL) was added and stirred for 2 hours. The final solution was sealed in a 30 mL Teflon-lined stainless steel autoclave, heated at 170°C for 7 days and then cooled to room temperature. After filtration and washing with distilled water, colorless crystals of **1** were obtained and dried in air (yield: *ca.* 80% based on H_3BO_3). IR bands (cm^{-1}) : 3613(w), 3531(s), 2355(w), 1647(w), 1374(s), 1306(s), 1244(s), 1082(m), 1062(m), 947(s), 872(m), 763(w), 729(m),701(m), 658(w), 583(w), 560(w), 489(m) and 433(w).

Preparation of $[C_5N_2H_{16}]AlB_5O_{10}$ (2)

Compound **2** was prepared using the same procedure as described for **1** with Al(*i*-PrO)$_3$ (0.204 g), H_3BO_3 (0.810 g), N,N'-bis(3-aminopropyl) ethylenediamine (0.50 mL) and pyridine (3.00 mL) except that colorless crystals of **2** were obtained at 180°C for 8 days (yield: *ca.* 90% based on H_3BO_3). Anal. Elemental analysis (%) calcd for $C_5H_{16}N_2AlB_5O_{10}$: C, 17.39; H, 4.63; N, 8.11. Found: C, 17.00; H, 4.34; N, 8.36. IR bands (cm^{-1}) : 3424(m), 3137(w), 2945(w), 1630(w), 1569(w), 1460(w), 1383(s), 1290(s), 1219(s), 1056(m), 928(s), 880(m), 756(w), 722(m), 696(m), 677(w), 627(w), 598(w), 476(m), 431(w).

Preparation of $[H_2dap][(CH_3)_2NH]AlB_5O_{10}$ (3)

Compound **3** was prepared using the same procedure as described for **1** with Al(*i*-PrO)$_3$ (0.204 g), H_3BO_3 (0.804 g), dap (3.00 mL), DMF (5.00 mL) and alcohol(2.00 mL). Pure, colorless crystals of 3 were collected in nearly 90% based on H_3BO_3. Anal. Elemental analysis (%) calcd for $C_5H_{20}N_3AlB_5O_{10}$: C, 16.53; H, 5.51; N, 11.56. Found: C, 16.64; H, 5.19; N, 11.55. IR bands (cm^{-1}) : 3504(w), 3426(m), 3238(w), 2091(w), 1614(m), 1560(m), 1424(s), 1385(s), 1301(s), 1208(s), 1052(s), 932(s), 870(m), 766(m), 720(s), 669(m), 449(m).

Single-crystal structure determination

The intensity data sets were collected on a Gemini A Ultra CCD with graphite-monochromated Mo-Kα radiation (λ= 0.71073 Å) in the ω scanning mode at room temperature. The absorption corrections were performed using the multi-scan program. The structures were solved by direct methods and refined by full-matrix least-squares on F^2 with the SHELXTL97 program.[14] The H-atoms of the organic ligands were geometrically placed and refined using a riding model. All atoms except for H-atoms and water molecules were refined anisotropically. Further details for the structural analyses are summarized in Table 1. The purities of the compounds were confirmed by XRD powder diffraction study (Fig. S1-3). The ICSD reference number for the compound **1** is 426917, and the CCDC numbers for 2 and 3 are 970782 and 970743, respectively.

Results and discussion

Structure descriptions of 1 and 2

Table 1 Crystal data and structure refinement for 1-3.

Compound	**1**	**2**	**3**
experimental formula	$H_8B_5O_{14}AlRb_2$	$C_5H_{16}N_2B_5O_{10}Al$	$C_5H_{19}N_3B_5O_{10}Al$
formula weight	483.97	345.23	362.26
Temperature (K)	293(2)	293(2)	293(2)
wavelength (Å)	0.71073	0.71073	0.71073
crystal system	Orthorhombic	Orthorhombic	Orthorhombic
space group	$C222_1$	$P2_12_12_1$	*Pbca*
a (Å)	10.3686(4)	9.5900(5)	13.1857(6)
b (Å)	9.5456(3)	10.3214(6)	13.2861(5)
c (Å)	14.0571(4)	13.7988(9)	17.3296(7)
V (Å^3)	1391.29(8)	1365.84(14)	3035.9(2)
Z	4	4	8
density (g/cm)	0.878	1.679	1.585
absorption coefficient(mm^{-1})	3.580	0.200	0.188
F(000)	345	378	1504
Crystal size (mm^3)	0.10 × 0.05 × 0.05	0.30 × 0.2 × 0.1	0.30 × 0.2 × 0.1
reflections collected	2834	4430	7433
unique reflections (R_{int}) refined	1196(0.0237)	2366(0.0182)	2697(0.0255)
parameters	103	210	217
Goodness-of-fit on F^2	1.017	1.078	1.265
R_1^a/wR_2^b [$I > 2\sigma(I)$]	0.0265 / 0.0664	0.0404 / 0.1070	0.0741/ 0.2052
R_1^a/wR_2^b (all data)	0.0278 / 0.0676	0.0439 / 0.1091	0.0845 / 0.2133

Single-crystal X-ray diffraction analysis reveals that both compounds **1** and **2** crystallize in noncentrosymmetrical space groups $C222_1$ and $P2_12_12_1$ respectively, and they exhibit similar 3D aluminoborate frameworks with intersecting 6, 8-MR helical channels and large odd 11-MR channels.

As shown in Fig. 1, the asymmetric unit of **1** contains one unique Rb atom, one Al atom and three B atoms in the asymmetric unit. Atoms Rb(1), B(1) and B(3) locate in general positions, while atoms Al(1) and B(2) occupy special positions with site multiplicity of 0.5 respectively. In the asymmetric unit of 2, however, there are 23 non-hydrogen atoms including one aluminum atom, five boron atoms, ten oxygen atoms, five carbon atoms and two nitrogen atoms. In both structures, the Al atoms are tetrahedrally coordinated, while the B atoms exhibit dual coordination modes, *i.e.* both trigonal and tetrahedral. As was observed in many open-framework metal borates, the connectivity of four BO_3 units and one BO_4 unit creates the typical pentaborate B_5O_{10} cluster, which is featured by two planar B_3O_3 rings that are almost perpendicular to each other. According to the crystal chemical classification scheme proposed by Heller, and Christ and Clark, such B_5O_{10} *FBB* can be expressed as (5:[(5:4Δ+T)]). The Al-O bond lengths are in the range 1.738(3)-1.742(2) Å (compound **1**) and 1.723(2)-1.734(2) Å (compound **2**); the O-Al-O bond angles are distributed in the range of 106.6(2)-113.8(2)° and 106.3(2)-111.2(2)° for **1** and **2** respectively. The B-O bond lengths for the BO_3 triangles [1.341(5)-1.392(5) Å for **1** and 1.327(4)-1.404(4) Å for **2**] are approximately shorter than those related to the BO_4 units [1.458(4)-1.477(4) Å for **1** and 1.459(4)-1.474(4) Å for **2**]. The O-B-O bond angles for BO_3 and BO_4 units are in the range of 117.4(3)-123.2(3)° and 108.0(4)-111.1(2)° for **1**, and 117.4(3)-122.8(3)° and 107.9(3)-111.3(2)° for **2**, respectively.

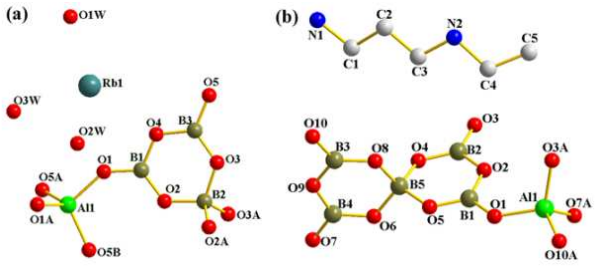

Fig.1 The asymmetric unit of compounds **1** (a) and **2** (b).

Compounds **1** and **2** are isomorphous, therefore, only the structure of **1** will be represented. In the construction of the open-framework, each AlO_4 unit is linked to 12 others through four bridging B_5O_{10} clusters, and each B_5O_{10} cluster is also connected to 12 others through four bridging AlO_4 units (Fig. S4). Thus, there is no Al-O-Al connection observed in the compound. This linkage mode gives rise to a 3D macroanionic $[Al(B_5O_{10})]_n^{2n-}$ framework with intersecting helical channels along the [100], [010] and [001] directions and large odd 11-MR channels along the [110] direction. Viewed down the [100] direction, two different channels that appear to have 6- and 8-ring apertures can be seen (Fig. 2). In fact, they are enclosed by two types of helices with opposite chirality. The left-handed helical chain is built from the infinite linkage of -AlO_4-BO_3-BO_3-AlO_4-BO_3-BO_3-AlO_4-BO_3-BO_3-, while the right-handed helical chain is built from the unclosed linkage of -AlO_4-BO_3-BO_4-BO_3-AlO_4-BO_3-BO_4-BO_3-AlO_4-BO_3-BO_4-BO_3-. These two types of helices with opposite chirality couple with each other to form the 3D framework with helical channels. Another type of helical channels with unclosed 6- and 8-MR openings can also be observed in the [010] direction, which are similar to those in the [100] direction, only differing in their shape and size. Along the [001] direction, however, larger helical channels are formed by the fusion of two unclosed right- and left-handed 8-ring apertures with -AlO_4-BO_3-BO_4-BO_3-AlO_4-BO_3-BO_4-BO_3-AlO_4- BO_3-BO_4-BO_3- sequence.

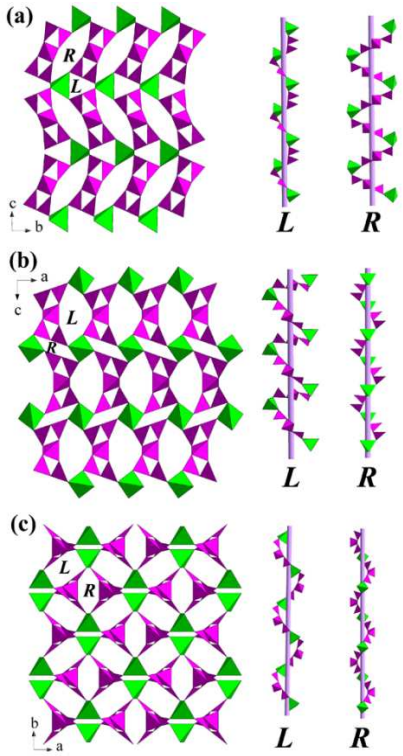

Fig.2 View of the 3D framework of **1** along the [010] (a), [010] (b) and [001] (c) directions showing intersecting helical channels (left), the left handed channels (middle) and the right-handed channels (right). Color code: AlO_4, green; BO_3 and BO_4, purple.

Besides the unclosed 6- and 8-MR helical channels, the presence of large odd 11-MR channels in the inorganic ABO framework makes another intriguing structural feature (Fig. S5). The pore size, defined by three AlO_4 tetrahedral, two BO_4 tetrahedral and six BO_3 triangles, has a free pore diameter of 6.7×10.9 Å (calculated from the oxygen-to-oxygen distance across the window, Fig. S6). Among the known zeotype inorganic materials, channels defined by rings containing large number of non-oxygen atoms (*e.g.* 9-, 11-, 13-, and 15-membered rings) are rarely observed. The presence of B_5O_{10} clusters may favor the formation of such channels. From the topological point of view, the 3D framework of the compound is a four-connected network if each AlO_4 group and each B_5O_{10} SBU acts as four-

connected nodes. The network is shown schematically in Fig. S7, and its Schäfli symbol is 6^6.

The extra-framework species: *i.e.* the Rb^+ cations and H_2O molecules in **1** and diprotonated $[NH_3(CH_2)_3NH_2CH_2CH_3]^{2+}$ cations in **2**, reside at the center of the 11-MR channels and simultaneously compensate for the negative charge of the macroanionic framework (Fig. S8). In **1**, the Rb atom is coordinated to eight oxygen atoms with Rb-O distances ranging from 2.927(4) to 3.430(2) Å. In **2**, the presence of new organic template $[NH_3(CH_2)_3NH_2CH_2CH_3]$ (*N*-ethyl-1,3-diaminopropane) is noteworthy, and it should be derived from the decomposition of initial N,N'-bis(3-aminopropyl)ethylenediamine. The decomposition of organic amines under hydro/solvothermal conditions was not unusual, and similar phenomenons were also observed during the syntheses of QD-2[12b] and AlPO4-GIS.[15] Extensive N-H···O type hydrogen bonds exist between the diprotonated organic molecules and the framework with N···O distances in the range of 2.908(4)-3.062(4) Å.

Structure descriptions of 3

Compound **3** crystallize in the orthorhombic space group *Pbca*, and the asymmetric unit contains one $[AlB_5O_{10}]^{5-}$ anion, one neutral dimethylamine and one diprotonated $[H_2dap]^{2+}$ cation. The occurrence of new dimethylamine molecule is noteworthy, and it derives from *in situ* hydrolysis of DMF solvent under present solvothermial conditions. As observed in compounds **1** and **2**, the typical $[AlB_5O_{10}]^{5-}$ anion is also composed of one AlO_4 tetrahedron and one B_5O_{10} cluster that are bridged by the common oxygen atom. The Al-O bond distances are in the range of 1.718(3)-1.739(3) Å, and the O-Al-O angles span from 107.36(14) to 111.69(15)°. The B-O distances vary from 1.322(5) to 1.390(5) Å and from 1.452(5) to 1.483(5) Å, and the the O-B-O bond angles are in the range of 115.8(3)-124.3(3)° and 106.9(3)-112.0(3)° for BO_3 and BO_4 units, respectively.

The overall 3D anionic framework of **3** is also built up from the same building blocks (AlO_4 and B_5O_{10} groups) as discussed in **1** and **2**. However, each AlO_4/B_5O_{10} cluster in **3** is connected to 11 B_5O_{10}/AlO_4 units (Fig. S9), forming a distinct 3D framework with intersecting channels. Fig.3a shows the single inorganic layer viewed down the [100] direction, showing the elliptical 14- and 8-ring apertures. The 8-ring window, composed of two AlO_4, two BO_4 and four BO_3 units in two repeating linkage of -AlO_4-BO_3-BO_4-BO_3-, has a pore size of ca. 4.5 × 7.7 Å (Fig. S10); the 14-ring window with a free diameter size of ca. 7.6 × 14.4 Å was defined by built from four AlO_4, two BO_4 and eight BO_3 units containing two repeating -AlO_4-BO_3-BO_3-AlO_4-BO_3-BO_4-BO_3- linkages (Fig. S11). Each 14-MR channel is surrounded by four 8-MR channels and vice versa. Such inorganic layers are stacked along the [010] direction in –ABAB–sequence (Fig.3b). Therefore, the elliptical 14-ring channels are not straight and they obviously blocked by those 8-ring windows. Along the [010] and [001] directions, however, large odd 11-MR channels can be seen (Fig.3c-f). In both cases, the 11-MR windows are made of three AlO_4, two BO_4, and six BO_3 groups in the linkages of AlO_4-BO_3-BO_4-BO_3-AlO_4-BO_3-BO_3-AlO_4-BO_3-BO_4-BO_3. Due to different –ABAB– stacking modes adopted between the neighboring layers, the openness of the 11-ring channels are distinct: almost fully overlapped along the *b* axis and severely blocked along the *c* axis. In order to clearly see packing modes, the topological repre-sentation of three building layers and corresponding packing modes are shown in Fig.4. If B_5O_{10} clusters and AlO_4 tetrahedra act as 4-connected nodes, the 3D framework has a CrB_4 topology with vertex symbols $4{\cdot}6^2{\cdot}6{\cdot}6{\cdot}6{\cdot}6$.

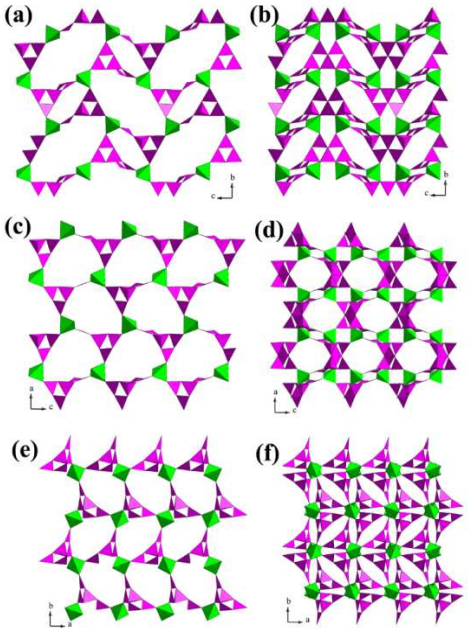

Fig. 3 Polyhedral views of the single inorganic layer (a, c, e), and the stacking of layers (b, d, f) of **3** along the [100], [010] and [001] directions, respectively. Color code: AlO_4, green; BO_3 and BO_4, purple.

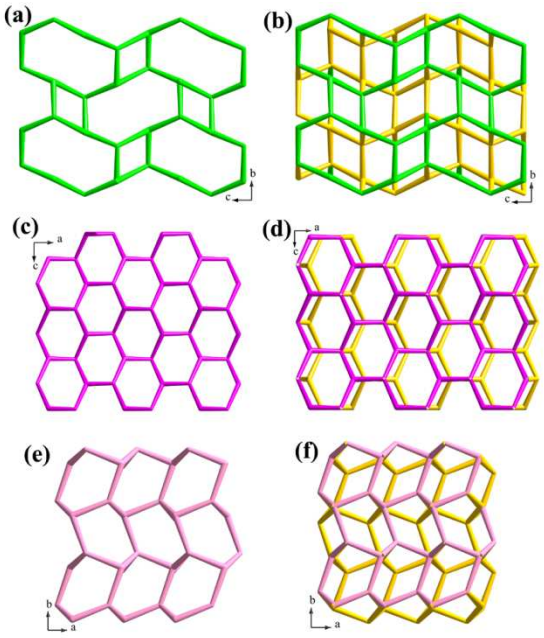

Fig.4 Topological representation of the single layer (a, c, e) and the stacking of layers (b, d, f) of **3** along the [100], [010] and [001] directions, respectively.

IR spectroscopy

The IR spectra of **1, 2** and **3** are were found to be comparable,

with minor differences between the spectra (Fig. S12). The strong bands in the range of 1208-1385 cm^{-1} (1244, 1306, 1374 cm^{-1} for **1**, 1219, 1290, 1383cm^{-1} for **2**, and 1208, 1301, 1385 cm^{-1} for **3**) are assigned to the BO_3 group, and the typical bands in the range of 1062-928 cm^{-1} (1062, 947 cm^{-1} for **1**, 1056, 928 cm^{-1} for **2**, and 1052, 932 cm^{-1} for **3**) are assigned to BO_4 group. The bands between 756 and 880 cm^{-1} (872, 763 cm^{-1} for **1**, 880, 756 cm^{-1} for **2**, and 870, 766 cm^{-1} for **3**) are assigned to the stretching vibrations of tetrahedral AlO_4 groups. The existences of organic templating agents in the structures are shown by the bands in the region 1460-1630 cm^{-1} for **2**, and 1424-1614 for **3**.

NLO, UV-Vis and Fluorescence Spectra Determination

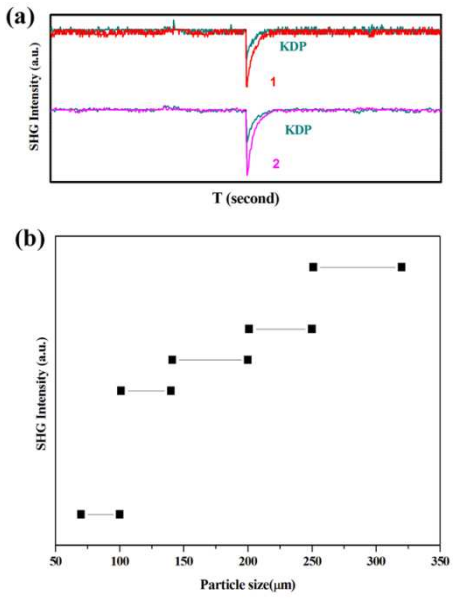

Fig.5 (a) Oscilloscope traces of the second harmonic generated signals KDP, **1** and **2**. (b) Phase-matching curve, that is, particle size vs SHG intensity for **1**.

Considering the noncentrosymmetric structural features of **1** and **2**, the second harmonic generation (SHG) measurements are carried out on their powder samples by the Kurtz-Perry method at room temperature. As shown in Fig.5a, both compounds display moderate SHG signals that are about 2.0 times the value of KH_2PO_4 (KDP) standard of a similar grain size, giving further evidences of their acentric structures. The phase matching curve of **1** is also shown in Fig.5b. According to the anionic group theory of NLO activity in borates,[16] it is believed that the SHG signals mainly originates from the BO_3 groups as well as small contributions from BO_4 groups. And the contributions from AlO_4 tetrahedra are also expected to be very small since their distortions are very small.

The UV-vis absorption spectral measurements indicate that **1-3** characteristic absorption peak are prominent at 250 nm, and there are no absorption between 250 and 1000 nm (Fig. S13). The good transmission property of the crystal in the entire visible region suggests its suitability for second harmonic generation.[17] Besides, according to the Kubelka-Munk function where $\alpha/S = (1- R)^2/2R$, optical diffuse reflectance studies reveal that the band gaps of **1-3** are approximately 3.8, 4.8 and 5.6 eV (Fig. 6), showing that they are wide-band-gap semiconductors.

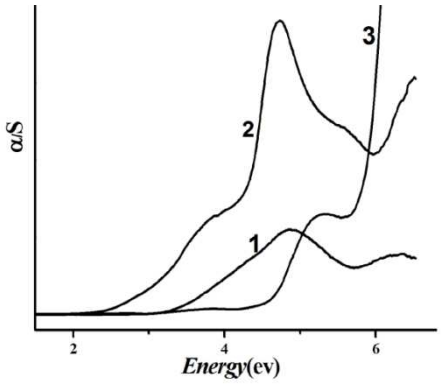

Fig. 6 UV-vis optical diffuse reflectance spectra for **1-3**.

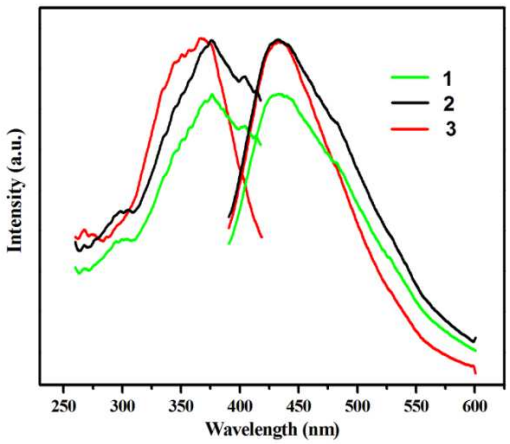

Fig. 7 Excitation and emission spectra of **1-3**.

The luminescence properties of **1-3** in the solid state were investigated at room temperature. As shown in Fig. 7, compounds **1-3** display blue photoluminescence with an emission maximum at about 433 nm upon excitation at 376, 376 and 367 nm, respectively. Although the three compounds contain different organic or inorganic cations in their channels, emission spectra shows they have almost the same emission intensity at 433 nm, which probably means that the fluorescence emission of these solids are not related to their template cations.

Thermogravimetric Analyses

To further study the thermal stabilities of compounds **1-3**, thermogravimetric analyses (TGA) were carried out at an air atmosphere from 30 to 1000°C with a heating rate of 10°C/min (Fig. S14). For **1**, the TG curve shows a weight loss of about 15% occurred in the temperature range 30-200°C, corresponding to the loss of the guest water molecules (calcd: 14.90%). For **2**, the structure can be stable to 205°C and then underwent three-step weight-loss processes in which the organic amines started to decompose. The total weight loss of 28.80% between 205-635°C should be attributed to the removal of organic amines (calcd: 29.56%). The structure collapsed and converted to an amorphous phase, suggesting that the framework was not stable to the ther-

mal removal of the template. For **3**, the TG curve shows a weight loss of 33.50% from 30 to 600℃, corresponding to the decomposition of organic amines (calcd: 33.42%).

Conclusion

In summary, three new 3D open-framework aluminoborates have been solvothermally synthesized and structurally characterized. Though constructed from the same B_5O_{10} clusters, the frameworks of **1**-**3** are quite different. Compounds **1** and **2** are isostructural and possess anionic framework with unusual intersecting helical channels and its Schäfli symbol is 6^6. Compound **3** is a co-templating open-framework aluminoborate with intersecting 8-, 11- and 14-ring channels and exhibit CrB_4 topology. Compounds **1** and **2** crystallize in acentric structures, and they have good NLO activity with SHG efficiency of about 2.0 times higher than that of KDP. Further work is in progress for making novel metal borate materials by using larger acentric B-O clusters and chiral Al, Zn, Ge, and Cd centers under hydro(solvo)thermal conditions.

Acknowledgements

This work was supported by the NSFC (nos. 91122028, 21221001 and 50872133), the NSFC for Distinguished Young Scholars (no. 20725101), the 973 program (nos. 2014CB932101 and 2011CB932504), A Project of Shandong Province Higher Educational Science and Technology Program (J13LD18) and the development project of Qingdao science and technology (13-1-4-187-jch).

Notes and references

[a]*MOE Key Laboratory of Cluster Science, Beijing Key Laboratory of Photoelectric/Electrophotonic Conversion Materials, School of Chemistry, Beijing Institute of Technology, Beijing 100081,China. E-mail: ygy@bit. edu.cn*;
[b]*Teachers College, College of Chemical Science and Engineering of Qingdao University, Shandong 266071, China. E-mail: gmwang_pub@163.com*;
[c]*State Key Laboratory of Structural Chemistry, Fujian Institute of Research on the Structure of Matter, Chinese Academy of Sciences, Fuzhou, Fujian 350002, China. E-mail: ygy@fjirsm.ac.cn*

1 (a) P.C. Burns, J.D.Grice and F. C. Hawthorne, *Can. Mineral.*, 1995, **33**, 1131; (b) P. C. Burns, *Can. Mineral.*, 1995, **33**, 1167; (c) J. D. Grice, P. C. Burns and F. C. Hawthorne, *Can. Mineral.*, 1999, **37**, 731.
2 (a) M. Touboul, N. Penin, G. Nowogrocki, *Solid State Sci.*, 2003, **5**, 1327; (b) H. Huppertz, B. von der Eltz, *J. Am. Chem. Soc.*,2002, **124**, 9376; (c) M.S. Wang, G.C. Guo, W.T. Chen, G. Xu, W.W. Zhou, K.J. Wu and J.S. Huang, *Angew. Chem. Int. Ed.*, 2007, **46**, 3909; (d) D.M. Schubert, M.Z. Visi, C. B. Knobler, *Inorg. Chem.*, 2008, **47**, 2017; (e) Z.E. Lin, G.Y. Yang, *Eur. J. Inorg. Chem.*, 2011, 3857; (f) Z. Y. Wu, P. Brandao, Z. Lin, *Inorg. Chem.*, 2012, **51**, 3088.
3 P. Becker, *Adv. Mineral.*, 1999, **37**, 979.
4 C. Chen, B. Wu, A. Jiang, G. You, *Sci. Sin. Ser. B (Engl. Ed.)* 1985, **28**, 235.
5 (a) C. Chen, Y. Wu, A. Jiang, B. Wu, G. You, R. Li, S. Lin, *J. Opt.Soc. Am. B* 1989, **6**, 616; (b) Y.Wu, T. Sasaki, S. Nakai, A. Yokotani, H. Tang, Chen, C. *Appl.Phys. Lett.* 1993, **62**, 2614; (c) C.T. Chen, Y.B. Wang, B.C. Wu, K.C. Wu, W.L. Zeng, L.H. Yu, *Nature*, 1995, **373**, 322; (d) H. Wu, S. Pan, K.R. Poeppelmeier, H. Li, D. Jia, Z. Chen, X. Fan, Y. Yang, J. M. Rondinelli, H. Luo, *J. Am. Chem. Soc.*, 2011, **133**, 7786; (e) H. Wu, H. Yu, S. Pan, Z. Huang, Z. Yang, X. Su, K. R. Poeppelmeier, *Angew. Chem. Int. Ed.*, 2013, **52**, 3406.
6 (a) R. P. Bontchev, J. Do and A. J. Jacobson, Angew. Chem., Int. Ed., 1999, **38**, 1937; (b) G.Y. Yang, S. C. Sevov, *Inorg. Chem.*, 2001, **40**, 2214; (c) P. W. Menezes, S. Hoffmann, Y. Prots, R. Kniep, *Inorg. Chem.*, 2007, **46**, 7503; (d) Y.X. Huang, Y. Prots, R. Kniep, Chem.-Eur. J., 2008, 14, 1757.
7 (*a*) A. Choudhury, S. Neeraj, S. Natarajan, C. N. R. Rao, *J. Chem. Soc., Dalton Trans.*, 2002, 1535; (*b*) D. M. Schubert, F. Alam, M. Z. Visi, C. B. Knobler, *Chem.Mater.*, 2003, **15**, 866; (*c*) A. K. Paul,K. Sachidananda, S. Natarajan, *Cryst. Growth Des.*, 2010, **10**, 456.
8 (a) M. S. Dadachov, K. Sun, T. Conradsson, X. D. Zou, *Angew. Chem., Int. Ed.*, 2000, **39**, 3674; (b) D.B. Xiong, H.H. Chen, M.R. Li, X.X. Yang, J.T. Zhao, *Inorg. Chem.*, 2006, **45**, 9301; (c) C.Y. Pan, G.Z. Liu, S.T. Zheng, G.Y. Yang, *Chem.-Eur.J.*, 2008, 14, 5057.
9 (*a*) C. J. Rijssenbeek, D. J. Rose, R. C. Haushalter and J. Zubieta, *Angew. Chem., Int. Ed. Engl.*, 1997, **36**, 1008; (*b*) M. M. Wu, T. S. C. Law, H. H. Y. J. Sung, W. Cai and I. D. Williams, *Chem. Commun.*, 2005, 1827.
10 Baerlocher, C.; Meier, W. M.; Olson, D. H. *Atlas of Zeolite Framework Types*; Elsevier: Amsterdam, The Netherlands, 2001.
11 (*a*) S. H. Yang,G. B. Li, J. Ju, Z. L. Yang, F. H. Liao,Y. X.Wang, J. H. Lin, *Inorg. Chim. Acta*, 2008, **361**, 2413; (*b*) T. Yang, J. L. Sun, L. Eriksson, G. B. Li, X. D. Zou, F. H. Liao, J. H. Lin, *Inorg. Chem.*, 2008, **47**, 3228; (*c*) W. L. Gao, Y. X. Wang, G. B. Li, F. H. Liao, L. P. You, J. H. Lin, *Inorg. Chem.*, 2008, **47**, 7080; (d) J. Ju, J.H. Lin, G.B. Li, T. Yang, H.M. Li, F.H. Liao, C.K. Loong, L.P. You, *Angew. Chem. Int. Ed.*, 2003, **42**, 5607; (e) T. Yang, A. Bartoszewicz, J. Ju, J.L. Sun, Z. Liu,X.D. Zou, Y.X.Wang, G.B. Li, F.H. Liao, B. Martin-Matute, J.H. Lin, *Angew. Chem. Int. Ed.*, 2011, **50**, 12555.
12 (a) G.M. Wang, J.H. Li, Z.X. Li, H.L. Huang, S.Y. Xue, H.L. Liu, *Inorg. Chem.*, 2008, **47**, 1270; (*b*) G.M. Wang, J.H. Li, H.L. Huang, H. Li, J. Zhang, *Inorg. Chem.*, 2008, **47**, 5039; (*c*) C. Rong, Z. Yu, Q.Wang, S.T. Zheng, C.Y. Pan, F. Deng, G. Y. Yang, *Inorg. Chem.*, 2009, **48**, 3650; (*d*) J. Zhou, S.T. Zheng, M.Y. Zhang, G.Z. Liu, G.Y. Yang, *CrystEngComm*, 2009, **11**, 2597; (*e*) J. Zhou, W.H. Fang, C. Rong, G.Y. Yang, *Chem. Eur. J.*, 2010, **16**, 4852; (*f*) G.J. Cao, J. Lin, J.Y. Wang, S.T. Zheng, W.H. Fang, G.Y. Yang, *Dalton Trans.*, 2010, **39**, 8631; (g) G.J. Cao, J. Lin, W.H. Fang, S.T. Zheng, G.Y. Yang, *Dalton Trans.*, 2011, **40**, 2940; (h) G.M. Wang, J.H. Li, P.Wang, Z.X. Li, Y.X. Wang, Z.M.Wang, J.H. Lin, *Dalton Trans.*, 2012, **41**, 734; (i) L.Z. Wu, L. Cheng, J.N. Shen, G.Y. Yang, *CrystEngComm* 2013, **15**, 4483; (j) W. Li, Q. Wei, Z.E. Lin, Q. Meng, H. He, B.F. Yang, G.Y. Yang, *Angew. Chem. Int. Ed.*, 2014, 53, 7188.
13 S. K. Kurtz and T. T. Perry, *J. Appl. Phys.*, 1968, **39**, 3798.
14 (*a*) G.M. Sheldrick, *Acta Crystallogr., Sect. A: Found. Crystallogr.*, 2008, **A64**, 112; (*b*) G.M. Sheldrick, *SHELXS-97, Program for Solution of Crystal Structures*University of Göttingen: Germany, 1997; (*c*) G.M. Sheldrick, *SHELXS-97, Program for Solution of Crystal Refinement*University of Göttingen: Germany, 1997.
15 J.L. Paillaud, B. Marler, H. Kessler, *J. Chem. Soc., Chem. Commun.*,1996, 1293.
16 C.T. Chen, Y.C. Wu, R.K. Li, *J. Cryst. Growth.*, 1990, **99**, 790.
17 A. Roshan, C. Joseph, M.A. Ittyachen, *Mater. Lett.*, 2001, **49**, 299.

Graphical Abstract:

Series of open-framework aluminoborates containing B_5O_{10} clusters

Li Wei,[a] Guo-Ming Wang[b,]*, Huan He,[a] Bai-Feng Yang,[a] Guo-Yu Yang*[a,c]